Max-Planck-Institut für Plasmaphysik

Excitation and damping mechanisms of Geodesic Acoustic Modes in tokamaks.

I. Novikau[1], A. Biancalani[1], A. Bottino[1], E. Poli[1], Ph. Lauber[1], P. Manz[1], G. D. Conway[1], L. Villard[2], E. Lanti[2], N. Ohana[2], ASDEX Upgrade Team[1]

(1) -Max-Planck-Institut für Plasmaphysik, Boltzmannstr. 2, 85748 Garching, Germany

(2) - École Polytechnique Fédérale de Lausanne, Swiss Plasma Center, Switzerland

HELMHOLTZ SPITZENFORSCHUNG FÜR GROSSE HERAUSFORDERUNGEN

EUROfusion

This work has been carried out within the framework of the EUROfusion Consortium and has received funding from the Euratom research and training programme 2014-2018 and 2019-2020 under grant agreement No 633053. The views and opinions expressed herein do not necessarily reflect those of the European Commission.

Introduction

- 2007-2012: Belarusian State University, Department of Physics, Department of Nuclear Physics:
  - Institute for Nuclear Problems, Flux Compression Generators, Internship
  - Institute of Applied Physics of the National Academy of Sciences of Belarus, Laboratory of computerized diagnostics (inverse problems, C++), Internship
- 2012-2014: The Joint Institute for Power and Nuclear Research - SOSNY, Nuclear Reactor Physics Laboratory, Research assistant:
  - DYN3D, EGSnrc Code System, FLUKA
  - automatic file processing (Java)
- 2014-2015: University of Lorraine, Institute of Jean Lamoure, Physics of Matter and Material Department:
  - Physics of High-Temperature Plasmas group, Internship
  - Implementation (with C++) of a code for 3D ideal MHD simulations in a slab geometry (Dr. Daniele Del Sarto)
- 2016-Present: Max Planck Institute of Plasma physics, Theory (TOK) department

Introduction & Motivation

- **Geodesic acoustic modes (GAMs)** [Winsor68 Phys. Fluids]: oscillatory counterparts of zero-frequency **Zonal Flows (ZFs)** [Hasegawa79 Phys. Fluids]

-> poloidally (m = 0) and toroidally (n = 0) symmetric radial electric field;
-> finite radial wavenumber;
-> GAM: geodesic curvature: m = 1 density oscillations;

- **Can reduce the radial transport**:

-> being excited by turbulence
-> as a sink for the turbulence energy
-> by shearing the vortices
-> role of the GAMs is still unclear [Scott03 Phys. Let. A]

- **Energetic particle (EP) driven GAMs (EGAMs)**: [Nazikian08 PRL, Fu08 PRL]

-> excitation via inverse Landau damping by energetic particles (EPs);
-> global radial structure;
-> interaction with turbulence [Zarzoso17 NF, Sasaki17 ScR].
-> bulk ion plasma heating by EPs through the EGAM [Sasaki11 PPCF, Osakabe14 IAEA, Wang19 NF];

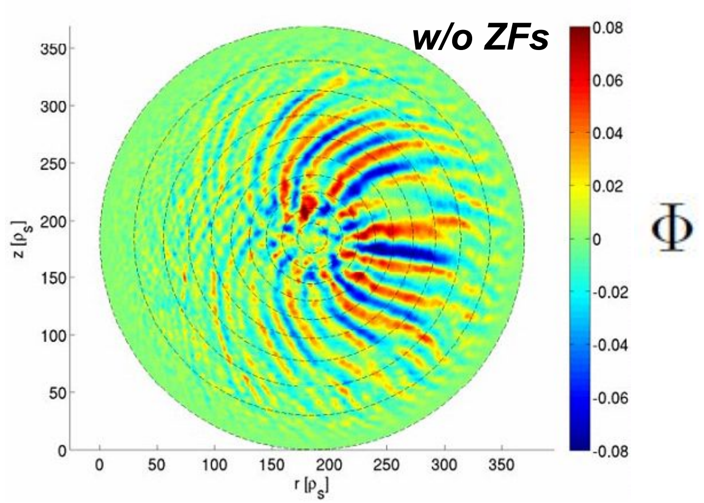

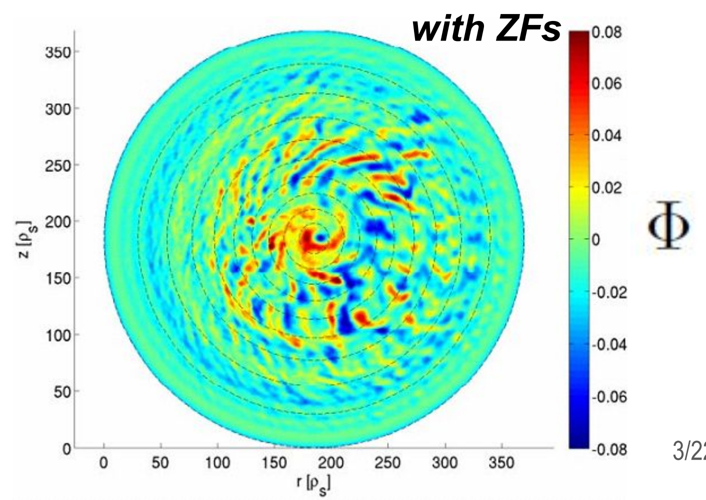

Outline

- ORB5 code
    - variational formulation
    - MPR diagnostic
    - Hamiltonian representation
- GAM: basics
- Electron damping of the GAMs
- EGAM dynamics in AUG shot
    - Mode chirping
    - plasma heating by EGAMs
    - Influence of electron dynamics
- Global GAM spectrum: staircase spectrum in AUG, global spectrum in TCV
- ITG-antenna as an externally applied field

ORB5 code [Jolliet07 CPC, Lanti19 CPC]

- ORB5 - gyrokinetic (GK) PIC code: global, EM.
- $\delta f_{sp} \rightarrow N_{sp}$ markers (sp - species with a charge $Z_{sp}e$ and mass m_{sp}).
- Marker position $(\boldsymbol{R}_{i,sp}, p_{i,sp}, \mu_{i,sp})$ and weight $w_{i,sp}, i = [i, N_{sp}]$.

$$\mathcal{A} = \int \mathrm{d}t \mathcal{L} = \sum_{sp} \int \mathrm{d}t\, \mathrm{d}V\, \mathrm{d}W \left(\underbrace{\boxed{\frac{Z_{sp}e}{c} \mathbf{A}^* \cdot \dot{\mathbf{R}} + \frac{m_{sp}c}{Z_{sp}} \mu \dot{\theta} - H_{0,sp} - H_{1,sp}}}_{L_{part}} \right) f_{sp}$$

$$\boxed{- \sum_{sp} \int \mathrm{d}t\, \mathrm{d}V\, \mathrm{d}W\, f_{0,sp} H_{2,sp}} - \boxed{\int \mathrm{d}t\, \mathrm{d}V \frac{|\nabla_\perp A_\parallel|^2}{8\pi}}$$

\- action functional of the ORB5 GK model

→ linearized decoupled Poisson and Ampère equations
→ $H_{2,sp}$ does not contribute to the particle equations of motion

→ no ES field energy
→ only perpendicular magnetic field perturbations are considered

$$\begin{aligned}
H_{0,sp} &= \frac{p_z^2}{2m_{sp}} + \mu B, \\
H_{1,sp} &= Z_{sp} e J_{0,sp} \phi - J_{0,sp} A_\parallel \frac{p_z}{m_{sp} c}, \\
H_{2,sp} &= -\frac{m_{sp} c^2}{2B^2} |\nabla_\perp \phi|^2 + \frac{(Z_{sp} e)^2}{2m_{sp} c^2} A_\parallel^2, \\
J_{0,e} &= 1.
\end{aligned}$$

No ordering assumptions on the perturbation of the distribution function:

$$f_{sp}(\mathbf{R}, p_z, \mu, t) = f_{0,sp}(\mathbf{R}, p_z, \mu) + \boxed{\delta f_{sp}(\mathbf{R}, p_z, \mu, t)}$$

→ sampled with markers

$$p_z = m v_\parallel + \frac{q A_\parallel}{c}$$

Hamiltonian representation

ORB5 code [Jolliet07 CPC, Lanti19 CPC]

$$\frac{\delta \mathcal{F}}{\delta \eta}\chi = \frac{\mathrm{d}}{\mathrm{d}\nu}\int F(\eta+\nu\chi, \nabla\eta+\nu\nabla\chi)\,\mathrm{d}\mathbf{r}\Big|_{\eta=0} = \boxed{\int \frac{\delta L}{\delta \eta}\chi\,\mathrm{d}\mathbf{r} + \int \frac{\delta L}{\delta \nabla\eta}\cdot\nabla\chi\,\mathrm{d}\mathbf{r}} =$$

- functional derivative

$$\boxed{\int\left(\frac{\delta L}{\delta \eta} - \nabla\cdot\frac{\delta L}{\delta\nabla\eta}\right)\chi\,\mathrm{d}\mathbf{r}} + \boxed{\int \nabla\cdot\left(\frac{\delta L}{\delta\nabla\eta}\chi\right)\mathrm{d}\mathbf{r}}$$

→ weak form

→ dynamical term to get field and particle equations of motion

→ Noether term to get conserved quantities (power balance)

$$\mathcal{F}[\eta] = \int F(\eta, \nabla\eta)\,\mathrm{d}\mathbf{r}$$

- arbitrary functional

$$\frac{\delta \mathcal{L}}{\delta \phi}\hat{\phi} = 0$$

→ Poisson (quasineutrality) equation

$$\frac{\delta \mathcal{L}}{\delta A_{\|}}\hat{A}_{\|} = 0$$

→ Ampère equation

$$\sum_{sp\neq e} Z_{sp}e\int \mathrm{d}V\,\mathrm{d}W\, f_{sp}J_{0,sp}\hat{\phi} - e\int \mathrm{d}V\,\mathrm{d}W\, f_e\hat{\phi} =$$

$$\boxed{\sum_{sp\neq e}\int \mathrm{d}V\,\mathrm{d}W\, f_{0,sp}\frac{m_{sp}c}{B^2}\nabla_\perp\phi\cdot\nabla_\perp\hat{\phi}}$$

→ linearized polarization density

→ since electrons are drift-kinetic, there is no electron contribution to the polarization density

Euler-Lagrange equation:

$$\frac{\mathrm{d}}{\mathrm{d}t}\frac{\partial L_{part}}{\partial \dot{\mathbf{Z}}} = \frac{\partial L_{part}}{\partial \mathbf{Z}}$$

$$\mathbf{Z} = (\mathbf{R}, p_z, \mu)$$

→ particle equations of motion

$$\begin{aligned}
\dot{\mathbf{R}} &= \frac{c\mathbf{b}}{qB_{\|}^*}\times\boldsymbol{\nabla}(H_0+H_1) + \frac{\partial(H_0+H_1)}{\partial p_z}\frac{\mathbf{B}^*}{B_{\|}^*},\\
\dot{p}_z &= -\frac{\mathbf{B}^*}{B_{\|}^*}\cdot\boldsymbol{\nabla}(H_0+H_1),\\
\dot{\mu} &= 0.
\end{aligned}$$

MPR diagnostic

→ From the Noether theorem (in electrostatic case) [Tronko16 PoP]:

$$\mathcal{E} = \sum_{sp} \int \mathrm{d}W\,\mathrm{d}V\,\left(f(H_0 + H_1) + f_0 H_2\right) = \underbrace{\boxed{\sum_{sp} \int \mathrm{d}W\,\mathrm{d}V \left(\frac{p_z^2}{2m} + \mu B\right) f}}_{\mathcal{E}_k} + \underbrace{\boxed{\sum_{sp} \int \mathrm{d}W\,\mathrm{d}V \left(\frac{1}{2} Z e J_0 \Phi\right) f}}_{\mathcal{E}_f}$$

$$\mathcal{P} = \frac{\mathrm{d}\mathcal{E}_k}{\mathrm{d}t} = -\sum_{sp} Ze \int \mathrm{d}V\,\mathrm{d}W (\cancel{f_0} + \delta f)\dot{\mathbf{R}}_0 \cdot \boldsymbol{\nabla}(J_0 \Phi)$$

- wave-particle energy transfer signal

for Maxwellian and two bumps-on-tail distribution functions

$$\underbrace{\frac{\mathrm{d}\mathcal{E}_k}{\mathrm{d}t} = -\frac{\mathrm{d}\mathcal{E}_f}{\mathrm{d}t}} \rightarrow \boxed{\gamma = -\frac{1}{2}\frac{1}{n_\omega T_\omega}\int_0^{n_\omega T_\omega} \frac{\mathcal{P}}{\mathcal{E}_f}\,\mathrm{d}t}$$

energy conservation

γ - wave damping (if $\gamma < 0$) or growth rate (if $\gamma > 0$).

Time integration on several n_ω wave periods T_ω.

Mode-Particle-Resonance (MPR) diagnostic: [Novikau19 CPC]

$$\boxed{\mathcal{P}_{sp} = -\frac{Z_{sp} e}{N_{sp}} \sum_{i \in V, \Delta W_{sp}} w_{i,sp} \dot{\mathbf{R}}_{0,i,sp} \cdot \boldsymbol{\nabla}(J_{0,sp}\Phi)\big|_i,}$$

- discretization: in a whole real space V and velocity bin ΔW_{sp}

$J_{0,sp}\Phi\big|_i$ - gyroaveraged ES potential perturbation at a position of a marker i.

$\dot{\mathbf{R}}_{0,i,sp}$ - unperturbed species characteristics for a marker i.

Hamiltonian (p_z) representation

Symplectic representation : keep $p_\parallel = mv_\parallel$ as a canonical momentum $\rightarrow$ no cancellation problem, but an implicit time integrator is required since $\dot{p}_\parallel = -\dfrac{\mathbf{B}^*}{B^*_\parallel} \cdot \boldsymbol{\nabla} H - \dfrac{e}{c}\dfrac{\partial J_0 A_\parallel}{\partial t}$

$A_\parallel$

Hamiltonian representation : use $p_z = mv_\parallel + \frac{Ze}{c} J_0 A_\parallel$ to get $L = (\ldots) \cdot \dot{\mathbf{R}} - H$. An explicit time integrator can be used since $\dot{p}_z = -\dfrac{\mathbf{B}^*}{B^*_\parallel} \cdot \boldsymbol{\nabla} H$.

In the MPR, $u = p_z/m$ is used as a parallel velocity coordinate: valid in ES ($\rightarrow p_z = mv_\parallel$) and EM low-$\beta$ ($\rightarrow p_z \approx mv_\parallel$) simulations.

For EM simulations with an arbitrary β, mixed-variable formulation can be used [Mishchenko19, CPC] , but requires calculation of $\dfrac{\partial J_0 A_\parallel}{\partial t}$ [Bottino20, to be subm. NJP] .

Cancellation problem appears:

$$-\nabla_\perp^2 A_\parallel = \mu_0 \sum j_\parallel^{kin} + \underbrace{\boxed{\mu_0 \sum j_\parallel^{adiab} - \sum_{sp} \frac{\beta}{\rho^2} J_0 \overline{A}_\parallel}}_{}^{\text{must be } = 0}$$

$\sum_{sp} \dfrac{\beta}{\rho^2} J_0 \overline{A}_\parallel \gg \nabla_\perp^2 A_\parallel \rightarrow$ exact cancellation is required.

$\rightarrow$ Control variates approach [Hatzky07, PoP] and the mixed-variable formulation [Mishchenko19, CPC] can be used to mitigate the problem.

GAMs: basics

- Appear due to the geodesic curvature of the background magnetic field in a tokamak.
- Frequency of order of a sound frequency ***cs / R***
- Landau damping - main damping mechanism of the mode

(also collisional mechanism, but mainly at the very edge)

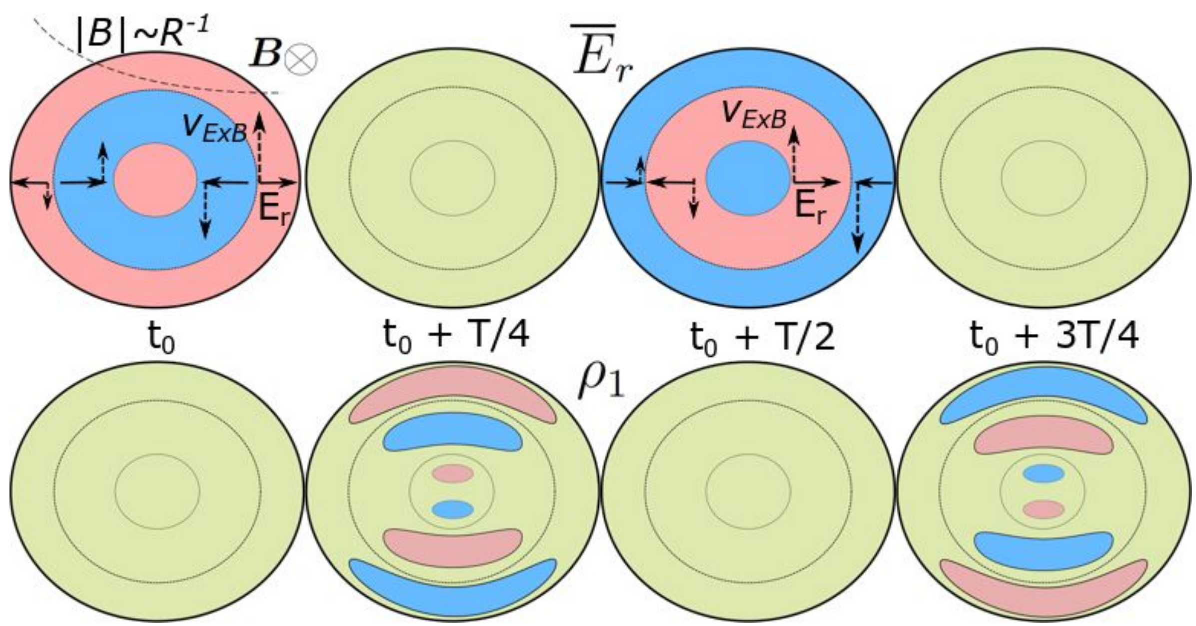

T - GAM period.

$\overline{E}_r$ - zonal electric field (flux-surface averaged, with $(n, m) = (0, 0)$ toroidal n and poloidal m modes).

ρ_1 - density perturbation (mainly, $(n, |m|) = (0, 1)$).

Electron Landau damping of GAMs

[Novikau17 POP]

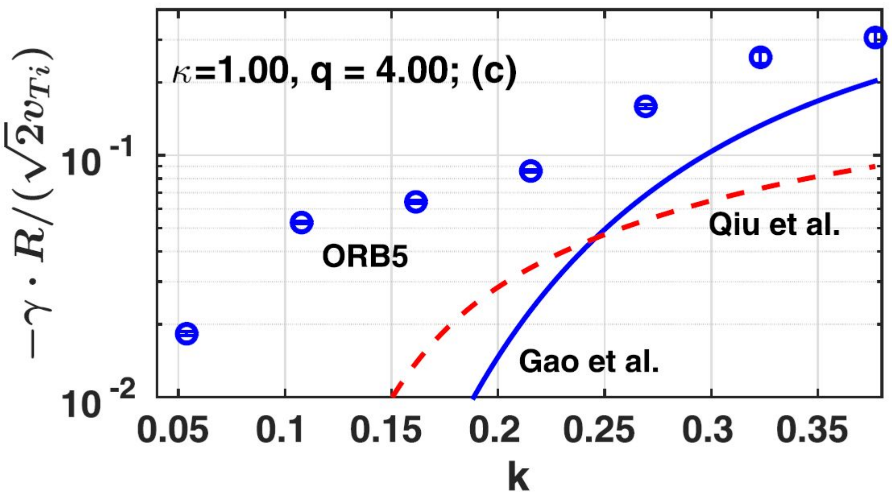

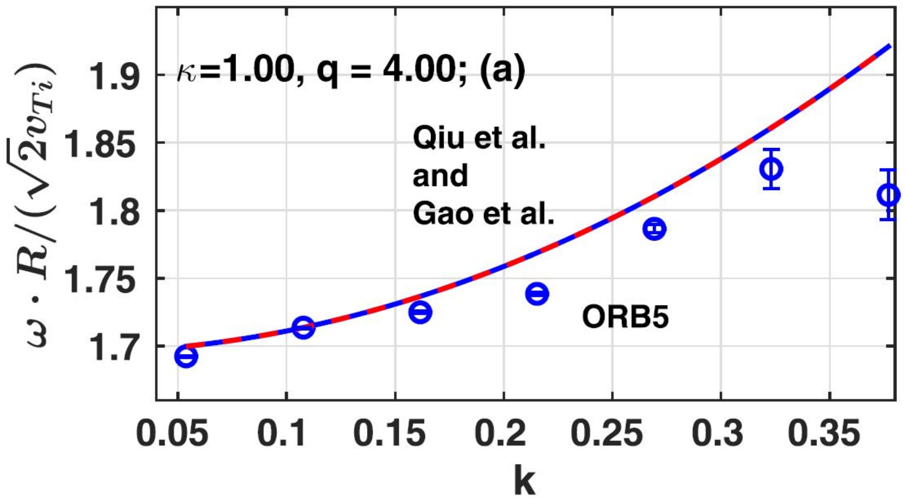

- GAMs are subject to electron Landau damping [Zhang10 PoP, Biancalani17 PoP]
- *B = 2 T, R = 1.65 m, a = 0.5 m*
- Inclusion of the electron dynamics:
  - GAM frequency does not change
  - Significant increase of GAM damping rate

blue dots → linear GK simulations with drift-kinetic electrons

solid and dashed lines → linear analytical estimation of GAM frequency and damping rate, based on the assumption of adiabatic electrons

Qiu et al. -> [Qiu09 PPCF]
Gao et al. -> [Gao10 POP]

AUG plasma configuration

- **ASDEX Upgrade shot #31213@0.84s.**
- EGAM chirping: branch 45-60 kHz
  with a period ~ 13 ms

Experimental spectrogram
[Horváth16 NF, Lauber18 IAEA]

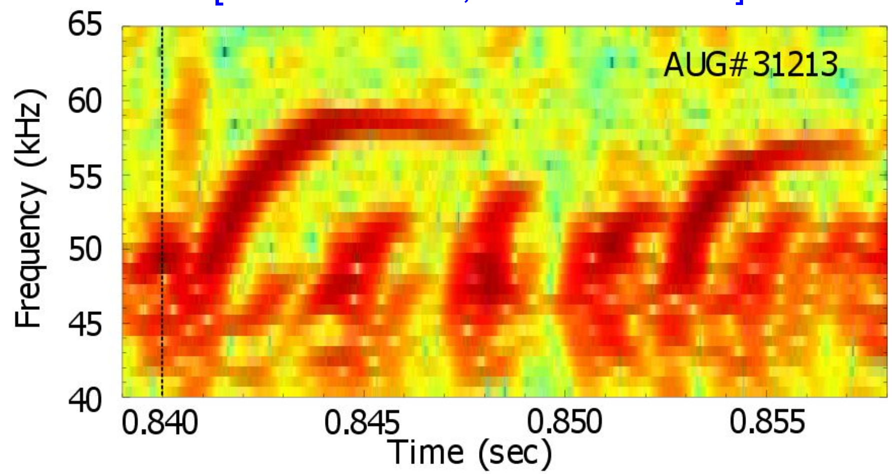

GK simulations:

- realistic magnetic configuration
- collisionless
- ES simulations with adiabatic electrons (AE)
- EM simulations with drift-kinetic electrons (KE)
- only n=0, |m| = [0,...,3] modes
- three species:
  gyrokinetic thermal deuterium
  thermal electrons (AE or KE)
  gyrokinetic energetic deuterium (EPs)
- no sources: relaxing EP distribution function

$$R_0 = 1.67\ m, \quad a_0 = 0.482\ m, \quad B_0 = 2.2\ T,$$

$$\beta_e = 2.7e-4, \quad \frac{m_d}{m_e} = 3672.$$

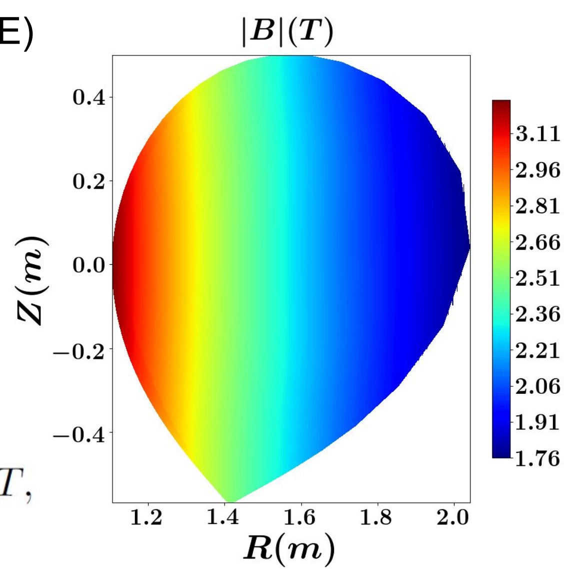

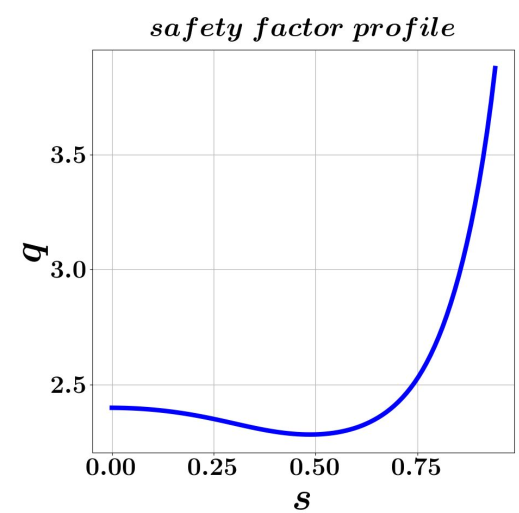

AUG plasma configuration

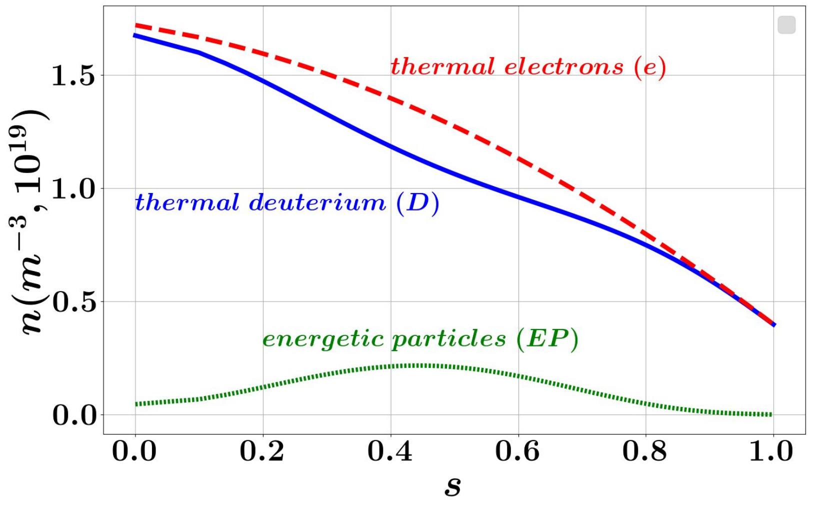

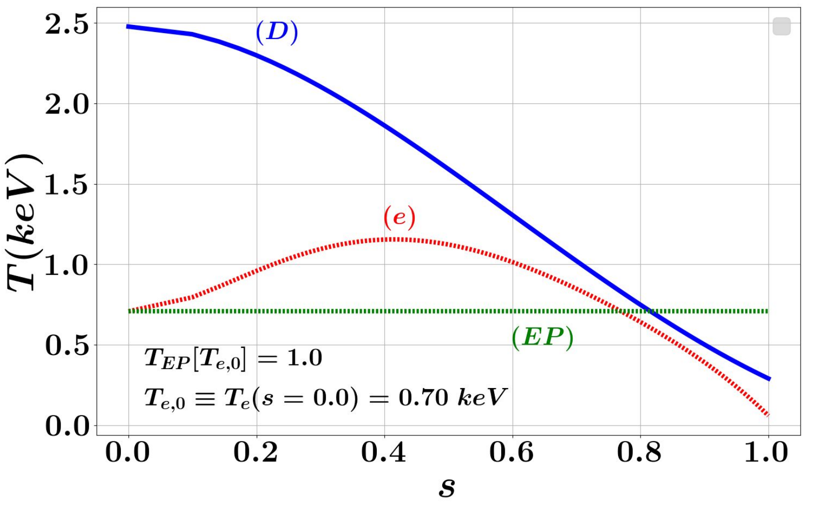

- realistic profiles
- model of EPs:
    - two shifted Maxwellians in velocity space.

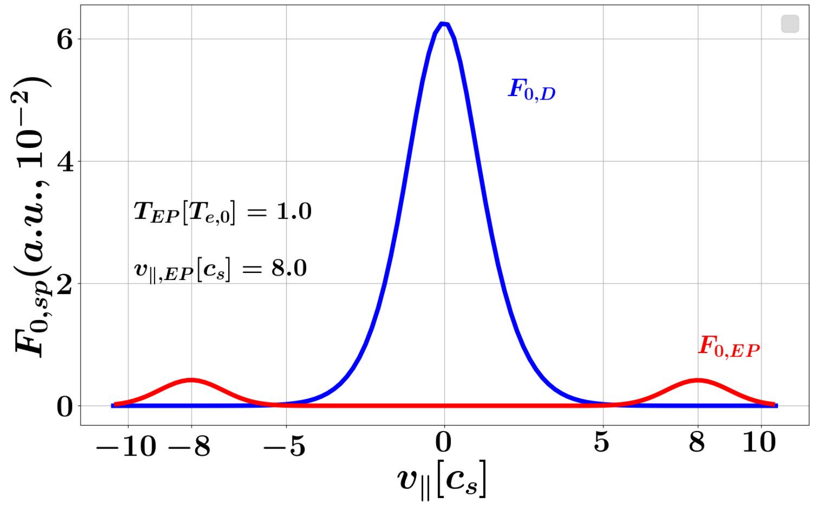

EGAM chirping and comparison with AUG experiment

GK ES NL simulation with AE

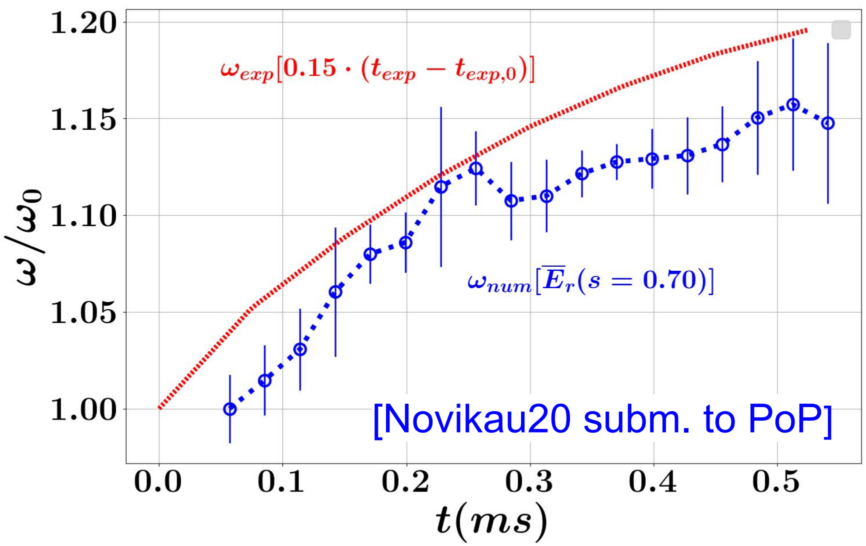

Experimental spectrogram [Horváth16 NF]

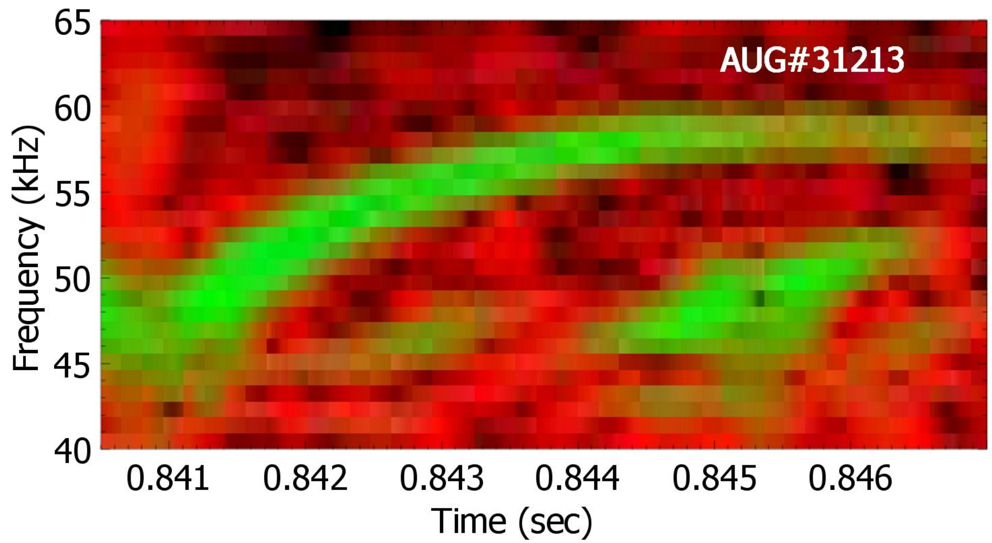

EP parameters: $v_{\parallel,EP} = 8.0$, $T_{EP} = 1.0$, $n_{EP}/n_e = 0.095$, - are taken in consistency with previous simulations: [DiSiena18 NF, Novikau19 CPC]

The numerical spectrogram is measured at the mode localisation radial point.

Comparable relative chirping of the mode.

Shift in EGAM frequency, overestimation of the chirping cycle time =>

necessary to use experimentally more accurate EP distribution function.

EGAM excitation

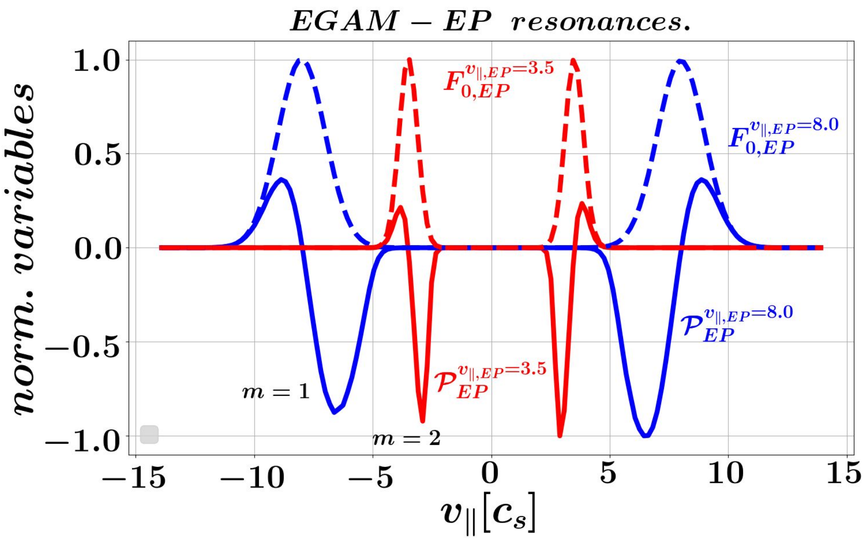

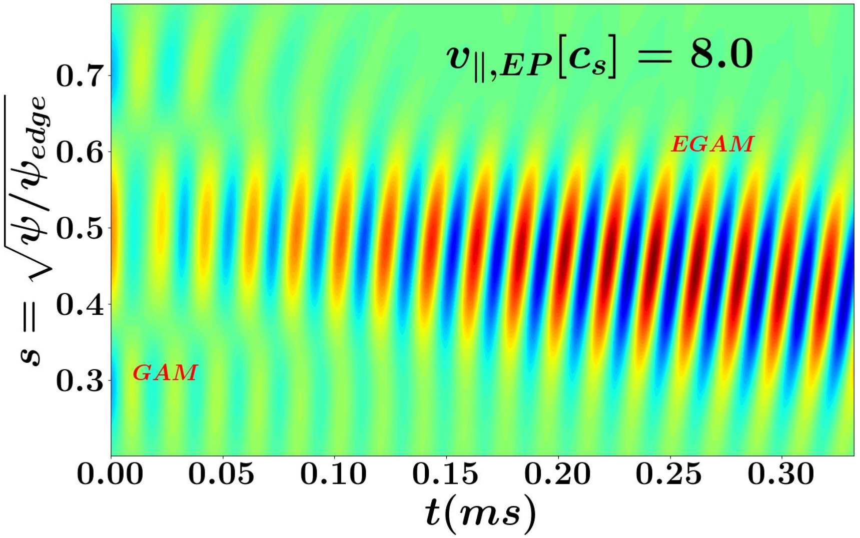

Linear ES simulations with AE.

- Simulation with $v_{\parallel,EP}[c_s] = 8.0$: $\omega_{egam} \sim \omega_{gam}$
- Simulation with $v_{\parallel,EP}[c_s] = 3.5$: $\omega_{egam} \sim \omega_{gam}/2$

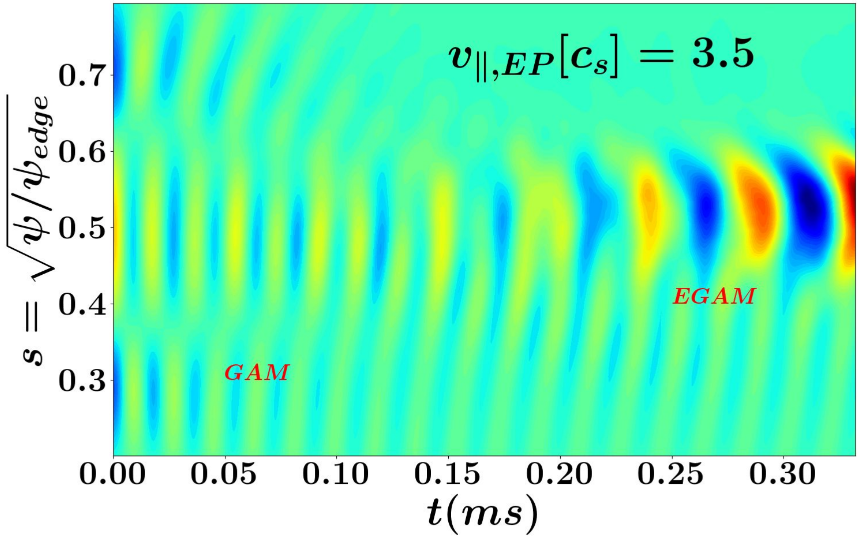

Localisation of the GAM-particle resonances:

$$v_{\parallel,res}^{(m)} = \frac{qR_0\omega_{gam}}{m}$$

Plasma heating by EGAMs

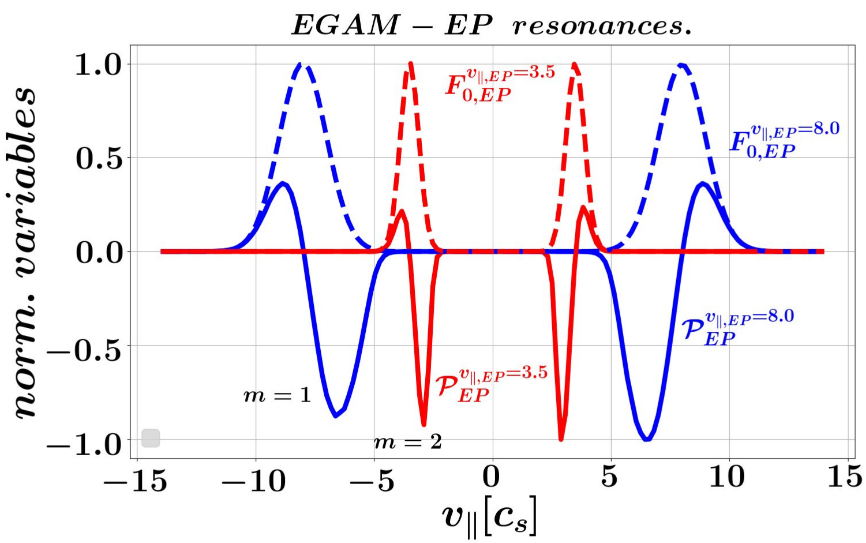

- Energy exchange between EGAM and thermal ions occurs **at high-order resonances** independently on the EP drive. Dominant m = 2 resonance.

- general **correlation** between the **EGAM level** and the **energy flow** to the thermal ions.

- **increased energy flow** due to high-order resonances.

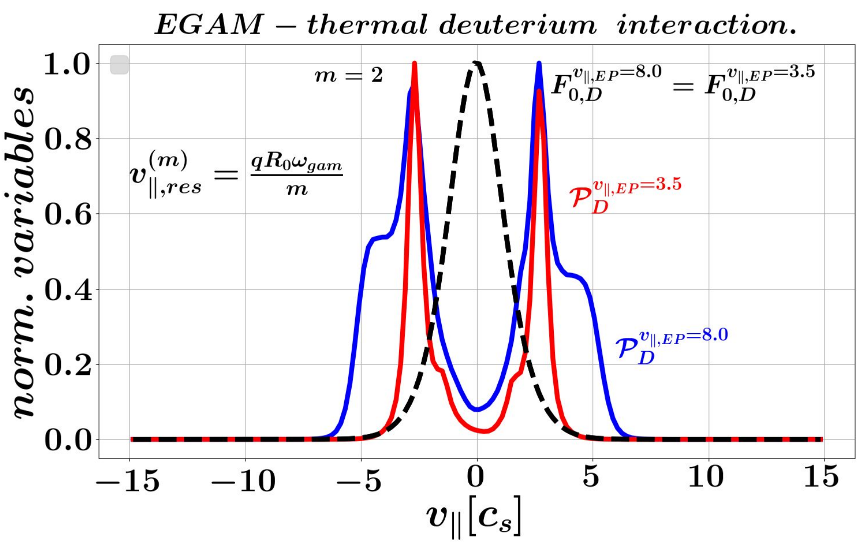

Linear ES simulations.

EGAM - Deuterium energy exchange *Versus* EGAM saturation levels

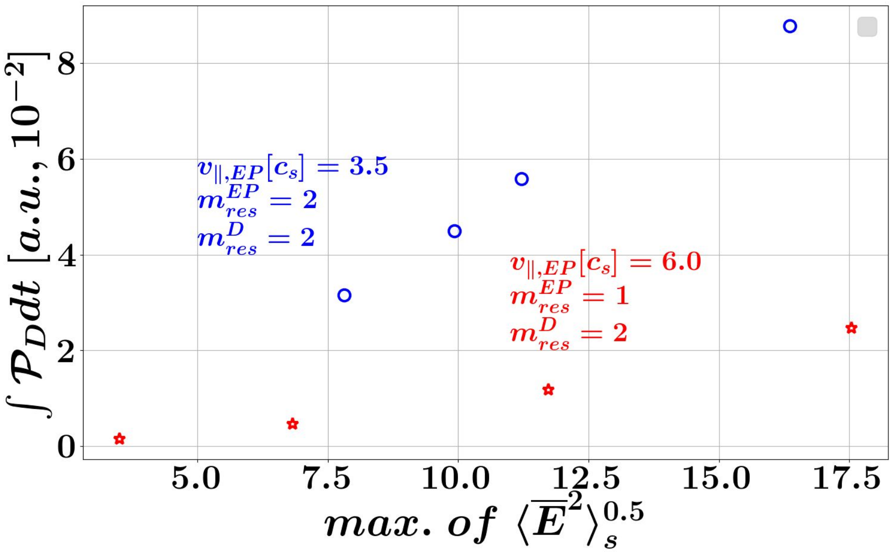

NL ES simulations

Role of electron dynamics

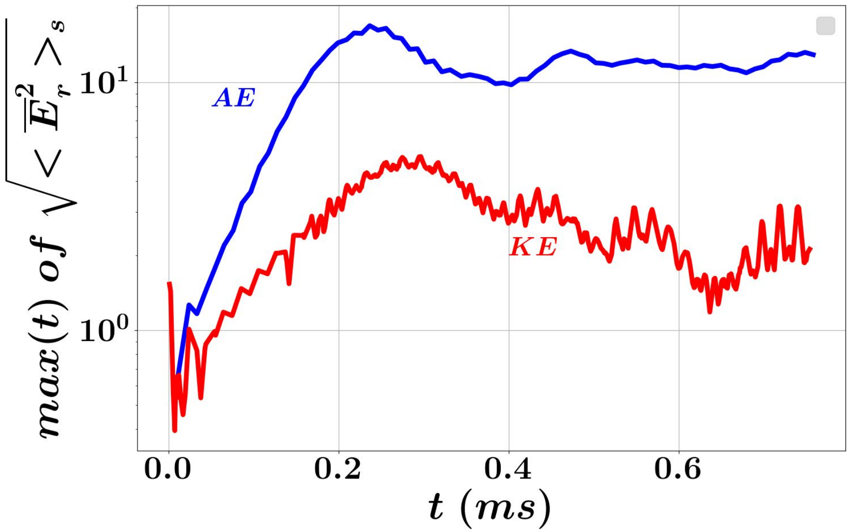

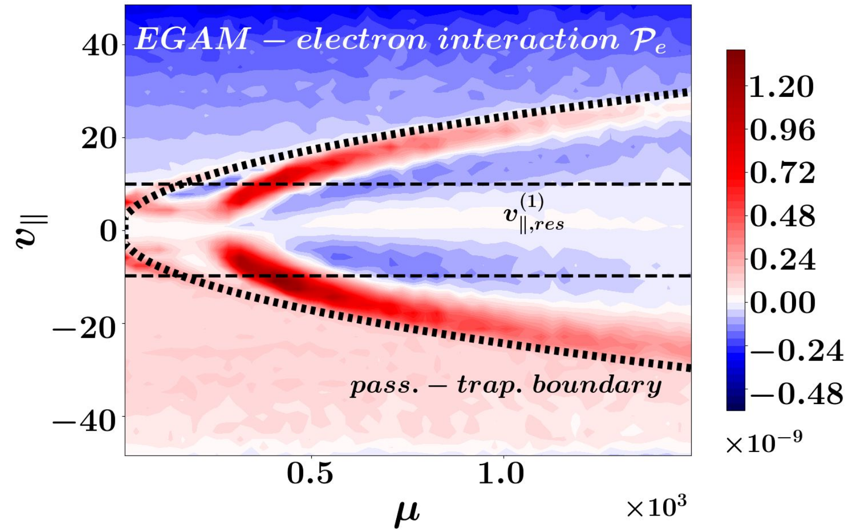

Nonlinear Electrostatic simulations with Adiabatic Electrons (AE)
versus
Electromagnetic simulations with drift-Kinetic Electrons (KE)

- Reduction of the EGAM saturation level due to the inclusion of the electron dynamics (consistent with the decrease of the EGAM linear growth rate **[Novikau19-CPC]**).

- EGAM resonance with barely trapped electrons

AUG #20787: Plasma configuration

- AUG#20787 shot [Conway08 PPCF]
- B = 2 T, R = 1.65 m, a = 0.5 m
- ES simulation with adiabatic electrons
- n = [0, 80], m = [-325, 325]
- s = [0.5, 1.0]
- Collisionless
- Reconstructed (from the experiment)

T, n radial profiles and plasma configuration.

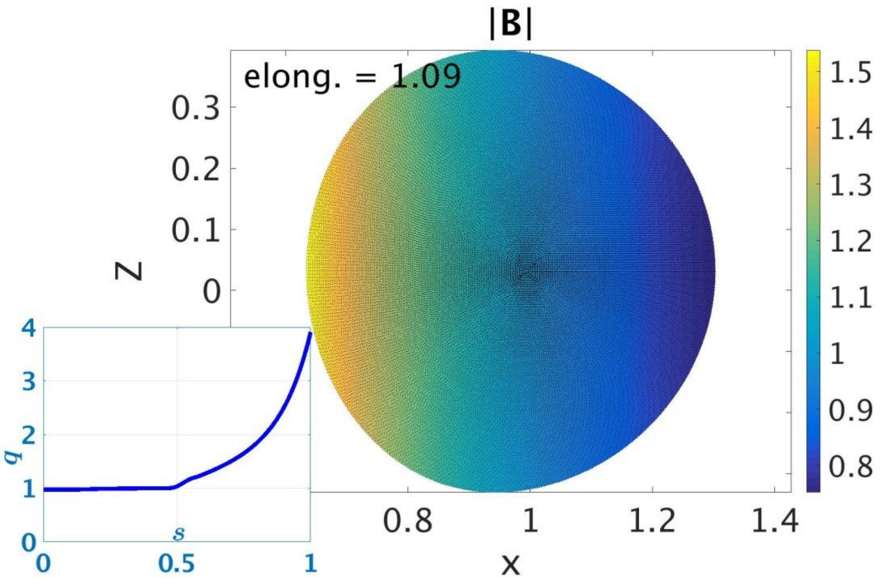

AUG #20787: GAM frequency scaling

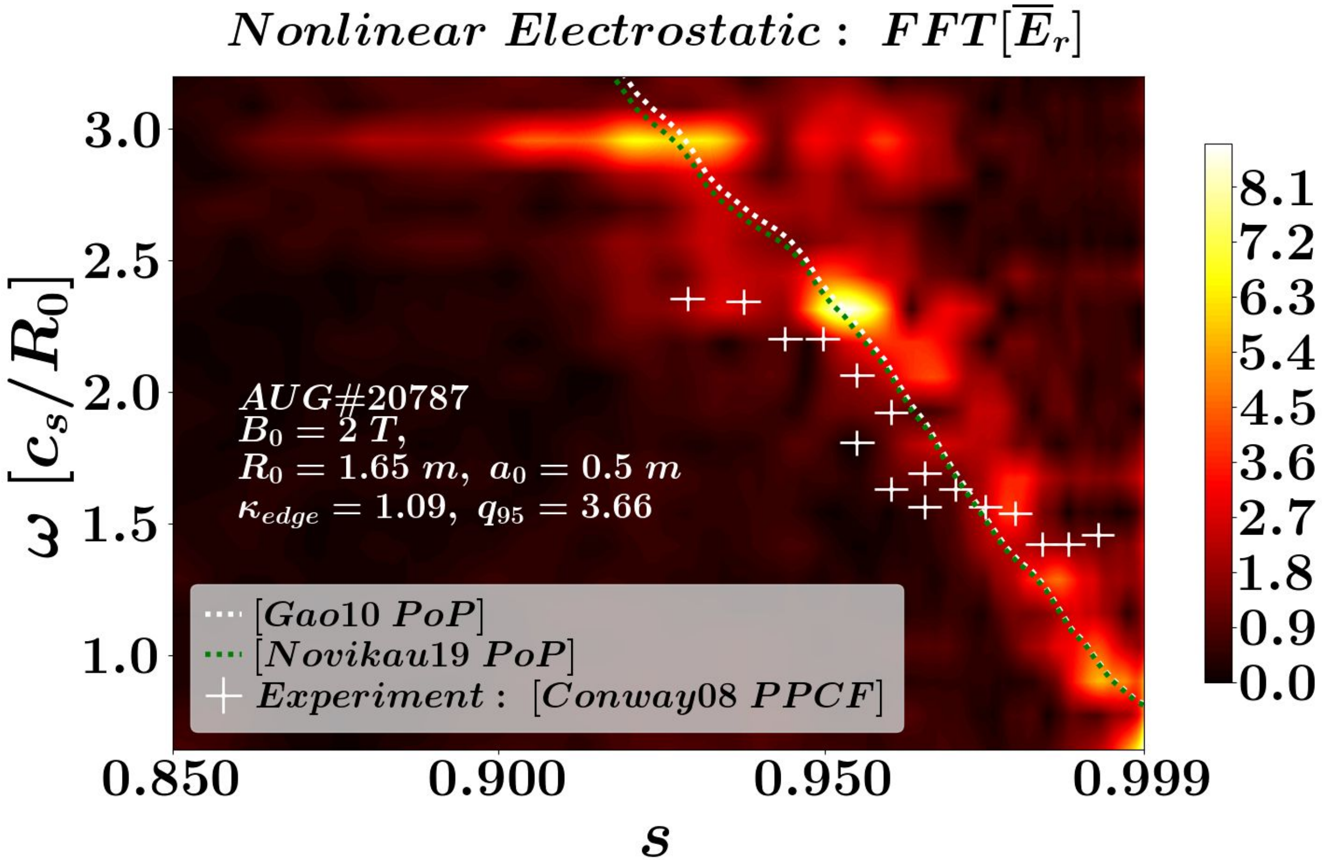

- Global GAM spectrum: coupling of m = 0 and m = 2 poloidal modes [Ilgisonis14 PPR].
- Plasma rotation enhances the global GAM formation [Lakhin15 PPR].
- Plasma rotation (e.g. due to NBI heating) or inclusion of kinetic electrons (TEM) might change the GAM spectrum.

GAMs in a TCV magnetic configuration

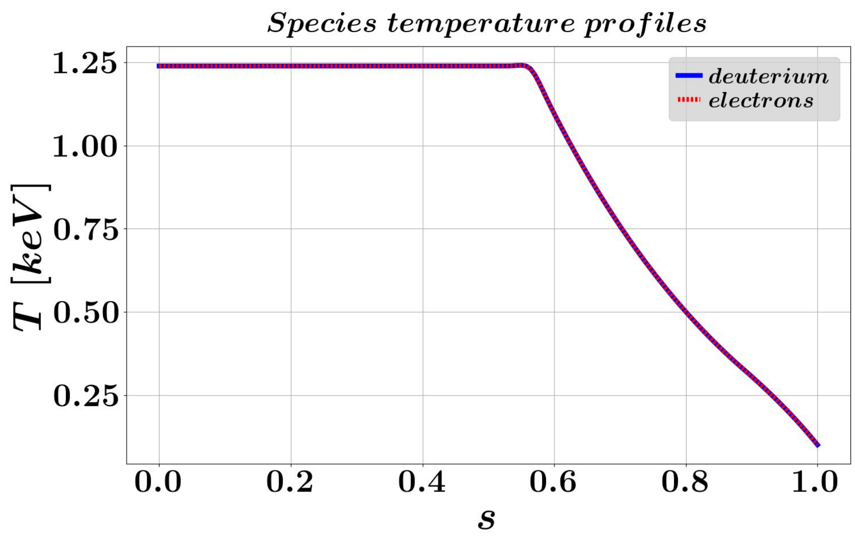

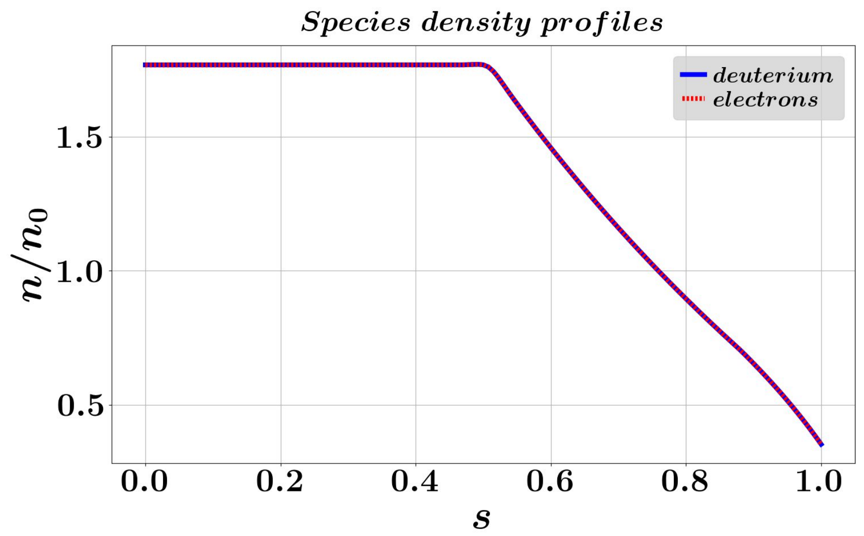

GK simulation in ORB5 of a TCV discharge:

- Electrostatic simulations with adiabatic electrons.

- realistic magnetic configuration;

- analytical temperature and density profiles;

- setting a relatively high temperature gradient at the edge, one observes global zonal structures **[Villard18-PPCF]**.

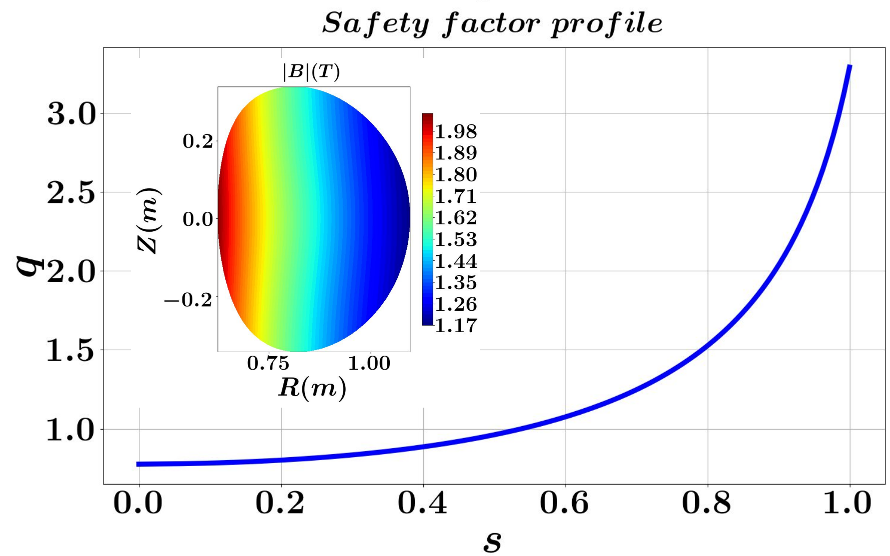

Global GAM-like structure

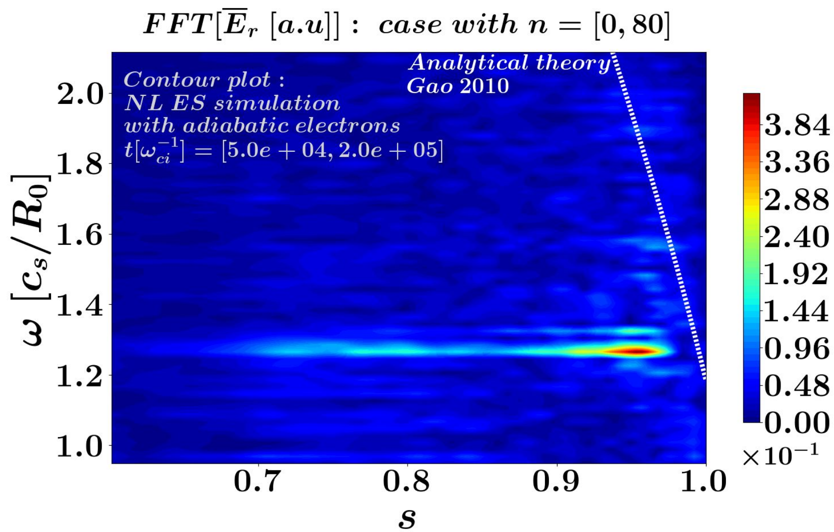

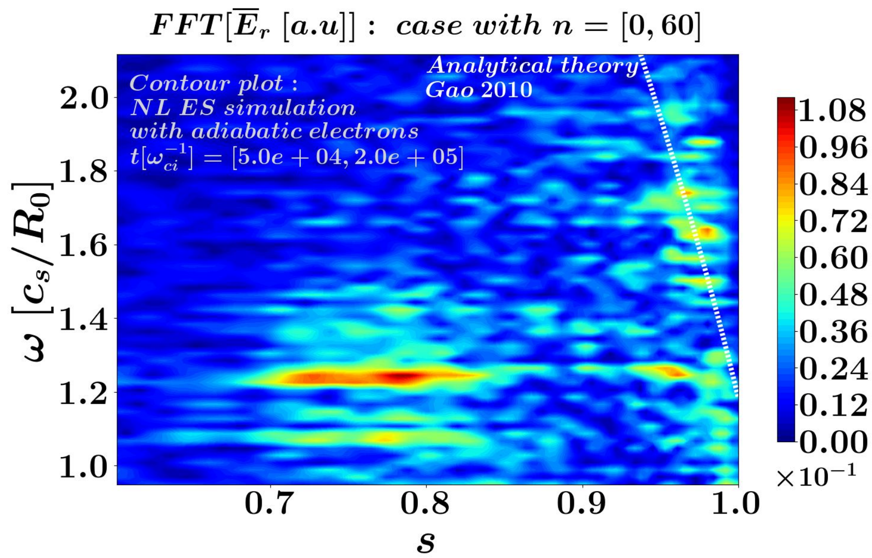

- Three GK simulations with different sets of the toroidal mode numbers *n*.

- Global structure (**s ~ [0.70, 0.98]**) with a frequency close to the GAM one **w ~ 1.2 [cs / R]** in spectra of the zonal electric field.

- Continuum GAM branch is also present.

- Presence of the global branch in the spectrum significantly depends on the turbulence spectrum.

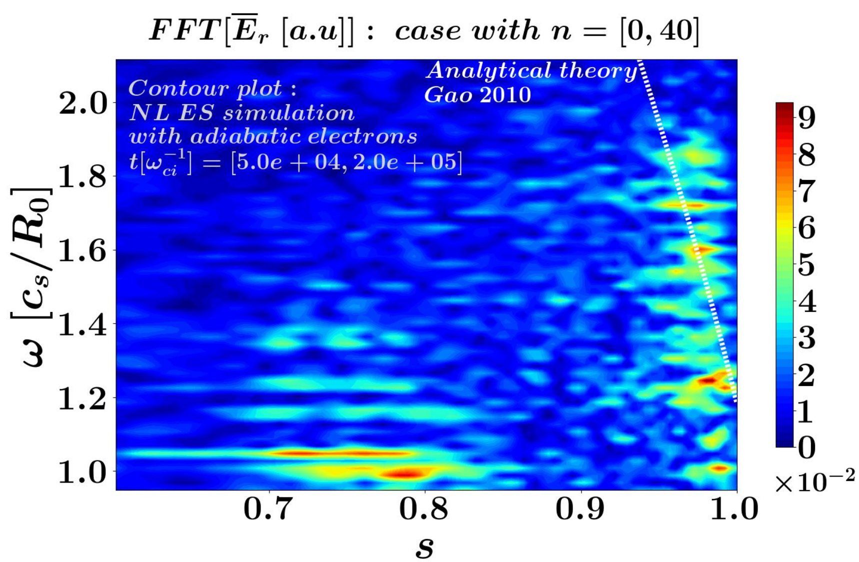

ITG-Antenna: in progress

Original simulation

Density perturbation

$\Downarrow$

Poisson equation

$\Downarrow$ $\Phi_{n,m}(s,t)$

Particle equations of motion

$$\dot{\boldsymbol{R}}_{sp}(\Phi),\ \dot{p}_{\|,sp}(\Phi)$$

$$\Phi^{ant}_{n_1,m}(s,t=t_1),\omega_{n_1}$$

Simulation with an antenna

Density perturbation

$\Downarrow$

Poisson equation

$\Downarrow$ $\Phi_{n,m}(s,t)$

Particle equations of motion

$$\dot{\boldsymbol{R}}_{sp}(\Phi,\Phi^{ant}),\ \dot{p}_{\|,sp}(\Phi,\Phi^{ant})$$

Take one n-mode (ES potential) with all possible m-modes:

- every m-mode has original radial structure;

- assume that all m-modes have the same frequency (one frequency for one n-mode).

$\Rightarrow$

GAM excitation by different ITG modes:

- realistic fixed ITG space structure taken from GK simulations
- dependence of the GAM growth rate on the ITG amplitude.
- GAM spectrum: continuum or global, dependence on a chosen n-mode or combinations of n-modes.

Zonal Antenna is already implemented in ORB5 **[Ohana18-JP]**.

Conclusions

- Mode-Particle-Resonance diagnostic has been implemented in ORB5.
- MPR diagnostic has been applied to a realistic AUG plasma configuration:
    - Electron damping is not negligible for both GAMs and EGAMs in AUG;
    - Localisation of the EGAM - **barely trapped electron** resonances.
- Nonlinear GAM excitation in AUG and TCV:
    - staircase GAM spectrum in AUG;
    - global spectrum in TCV.
- ITG antenna with a realistic space structure.

Outlook

- Electromagnetic version of the MPR diagnostic (using the mixed-variable approach).
- Extension of the GK code ORB5 with an experimentally more accurate EP distribution function (slow-down with a pitch angle dependence).
- Application of the ITG-antenna in different plasma regimes to investigate excitation of Zonal Structures (ZFs and GAMs).

Additional slides

ZF and GAM: NL excitation

- Zero frequency Zonal Flows (ZFs): non-linear excitation by drift-waves (DWs): modulation instability (four wave coupling);
- ZFs: different from mean ***ExB*** flows: must vanish if DWs drive is extinguished;
- GAM excitation: three wave coupling;
- Inverse cascade of energy: energy transfer from big $\boldsymbol{k_r}$ (small vortices) to small $\boldsymbol{k_r}$ (big patterns).

Primary (pump) drift wave: $\hat{k}_d,\ \omega_d$
ZF (modulating signal or envelop modulation): $\hat{k}_{ZF},\ \omega_{ZF}$; $\omega_d \gg \omega_{ZF}$
Sidebands (beat modes): $\hat{k}_{d+},\ \hat{k}_{d-}$; $\hat{k}_{d+} = \hat{k}_{ZF} + \hat{k}_d$ $\hat{k}_{d-} = \hat{k}_{ZF} - \hat{k}_d$

Pump DW + ZF -> generation of the Sidebands;
Sidebands + pump DW -> amplification of the ZF.

Electron Landau damping of GAMs

[Novikau17 POP]

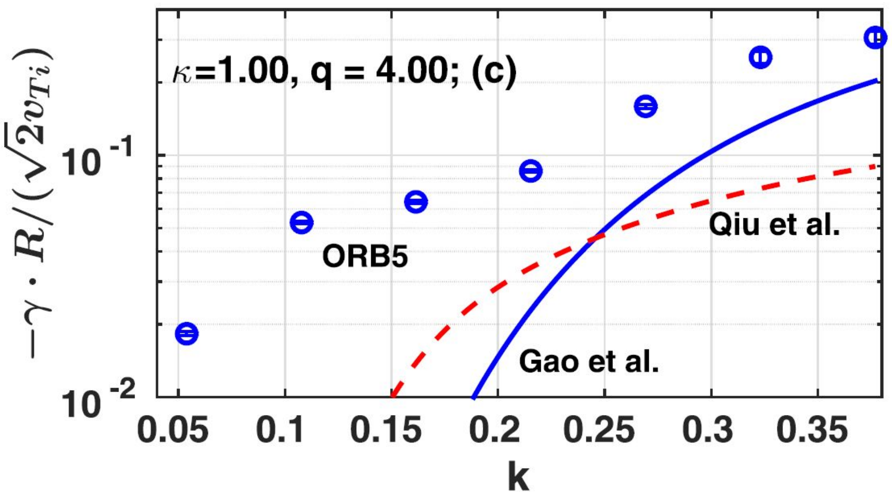

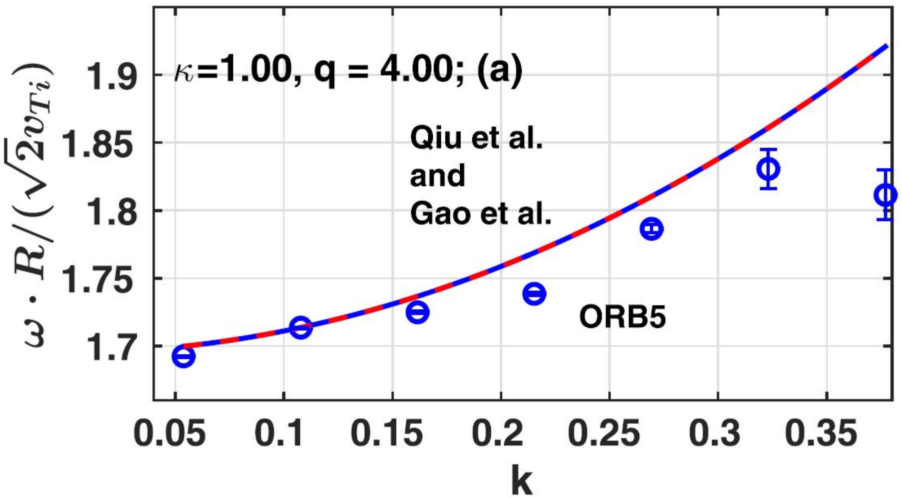

- Inclusion of the electron dynamics:
  - GAM frequency does not change
  - Significant increase of the GAM damping rate
- GK scan on radial wavenumber k, safety factor q, elongation κ -> fitting expressions for the GAM frequency f_ω and damping rate f_γ

g_i, h_i - known constant coefficients

$$f_\omega\left[\frac{\sqrt{2}v_{Ti}}{R}\right] = \frac{g_1 + g_2k^2 + g_3k^4}{1 + g_4k}\,\frac{\exp\left(-g_5q^2\right)}{1 + g_6\kappa}.$$

$$f_\gamma\left[\frac{\sqrt{2}v_{Ti}}{R}\right] = \frac{(h_1 + h_2k^2)\exp\left[-h_3q^2\right]}{1 + h_4\kappa^2} + \frac{(h_5 + h_6k^2)\exp\left[-h_7q^2\right]}{1 + h_8\kappa^4}$$

Qiu et al. -> [Qiu09 PPCF], Gao et al. -> [Gao10 POP]: analytical theories with an assumption of adiabatic electrons

MPR: Analytical verification (I)

$$z + q^2 \left(F(z) - \frac{N^2(z)}{D(z)} \right) = 0$$

GAM dispersion relation [Zonca96 PPCF, Zonca08 EL]
with $z = \frac{\hat{\omega}}{\omega_t}, \ \omega_t = v_{th}/(qR_0), \ v_{th} = \sqrt{2T/m},$

$$\hat{\omega} = \omega^D + i\gamma^D$$

complex GAM frequency consistent with the GAM dispersion relation

$$\overline{E}_r = \overline{E}_{r,1} \cos(kr) \exp(-i\hat{\omega}t)$$

correspondent evolution of the zonal electric field of the GAM

$$\delta f = \frac{e}{T} \frac{i\hat{\omega} F_0}{\hat{\omega}^2 - \omega_{tr}^2} \left(\frac{2cT}{eB_0 R_0} \frac{N(z)}{D(z)} - v_d \right) \overline{E}_r \sin\theta_p$$

$$\omega_{tr} = v_{\parallel}/(qR_0)$$

perturbation of the plasma distribution function consistent with the GAM dispersion relation

$$\dot{\mathbf{R}}_0 \cdot \mathbf{E} \approx \dot{\mathbf{R}}_0 \cdot \overline{\mathbf{E}} = -v_d \overline{E}_r \sin\theta_p$$

$$\mathcal{P} = \int \mathrm{d}V \, \mathrm{d}W \, e \delta f \dot{\mathbf{R}}_0 \cdot \mathbf{E} \approx i\hat{\omega} \frac{2mc^2}{B_0^2} \int \overline{E}_r^2 \sin^2\theta_p \, \mathrm{d}V$$

$$\mathcal{E}_{mode} = \frac{1}{2} \int \mathrm{d}V \, \mathrm{d}W \, e \delta f \Phi \approx \frac{mc^2}{2B_0^2} \int \mathrm{d}V \overline{E}_r^2$$

energy transfer signal and GAM energy derived using evolution of the density and zonal electric field perturbations, which are consistent with the GAM dispersion relation

$$\gamma^{MPR} = -\frac{1}{2} Re \left[\frac{\mathcal{P}}{\mathcal{E}_{mode}} \right] = -Re\left[i\hat{\omega} \right] = \gamma^D$$

MPR: Analytical verification (II)

Compare time evolution of the energy transfer signals, obtained from:

- ➔ ORB5 (from ES simulation of GAM with q = 1.5)
- ➔ the analytical derivation (using the GAM dispersion relation).

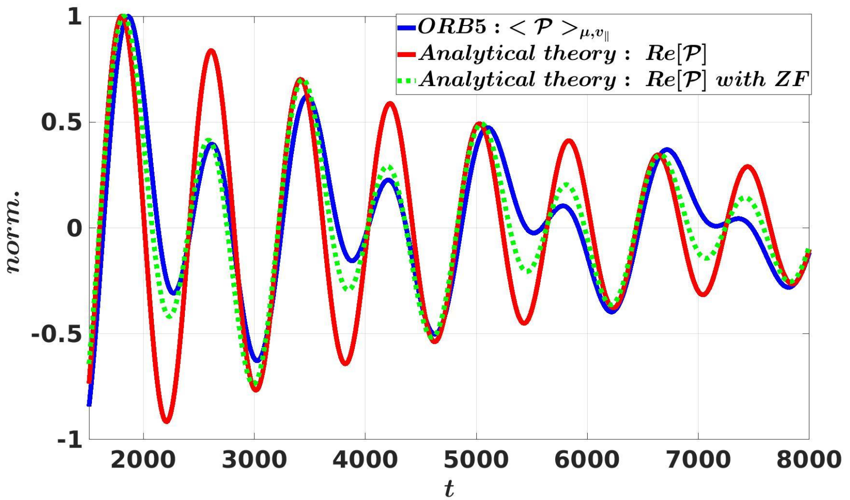

Energy transfer signal from ORB5 - blue line.

Analytical prediction, where only oscillatory part (GAM) of the radial electric field is taken into account: red line

$$\mathcal{P}_{real} \sim Re[\delta f] Re[\dot{\mathbf{R}}_0 \cdot \overline{\mathbf{E}}_r] \sim (\omega \sin(2\omega t) - \gamma - \gamma \cos(2\omega t)) \exp(2\gamma t)$$

$$\overline{E}_r = \overline{E}_{r,1} \cos(kr) \exp(-i\hat{\omega} t)$$

Analytical prediction, where constant component (Zonal Flow) is taken into account as well: green dashed line

$$\mathcal{P}^{ZF}_{real} \sim \frac{E_{r,0}}{E_{r,1}} (\omega \sin(\omega t) - \gamma \cos(\omega t)) \exp(\gamma t)) + (\omega \sin(2\omega t) - \gamma - \gamma \cos(2\omega t)) \exp(2\gamma t)$$

$$\overline{E}_r = \overline{E}_{r,0} + \overline{E}_{r,1} \cos(kr) \exp(-i\hat{\omega} t).$$

Linear EGAMs: NLED AUG plasma configuration

- AUG shot #31213 at 0.841 s [Lauber, AUG test case description#31213@0.84s (website) , Horva'th16 Nucl. Fusion, Di Siena18 Nucl. Fusion]
- B = 2.2 T, R = 1.66 m, a = 0.48 m
- Reconstructed (from the experiment)

T, n radial profiles and plasma configuration.

Three species: thermal deuterium, thermal electrons (adiabatic or drift-kinetic), energetic deuterium.

Energetic particle distribution:
two bumps-on-tail
-> not realistic
-> maximum numerical EGAM growth rate

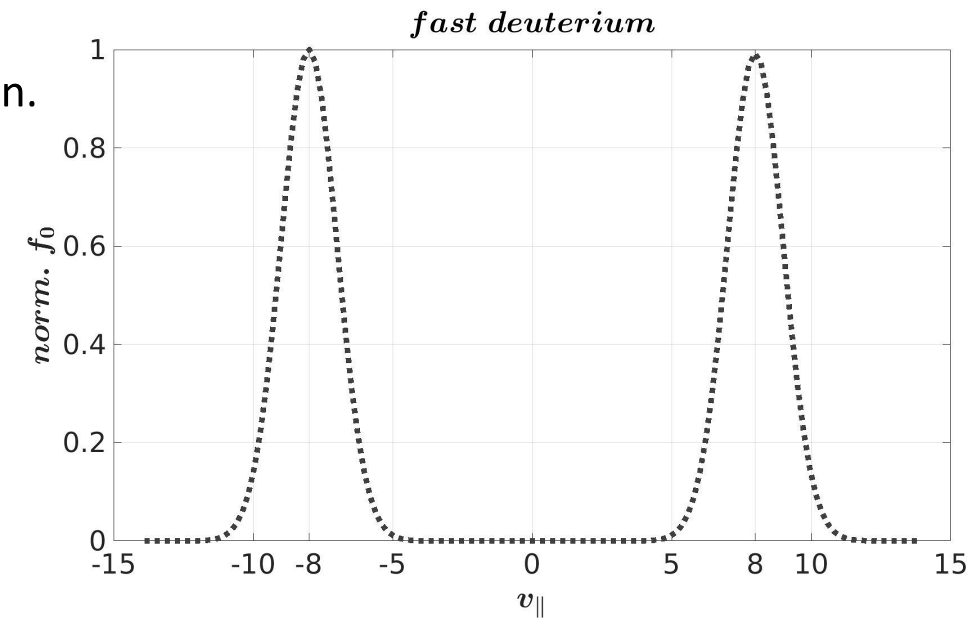

Sim. with adiabatic electrons:
-> ES
-> $dt[\omega_{ci}^{-1}] = 20$

Sim. with drift-kinetic electrons:
-> EM $\beta_e = \langle n_e \rangle T_e / (B_0^2/(2\mu_0)) = 2.7 \cdot 10^{-4}$
-> $dt[\omega_{ci}^{-1}] = 5$
-> realistic electron mass:
me/mi = 0.00027

Linear EGAMs in the NLED-AUG: wave-particle interaction (I)

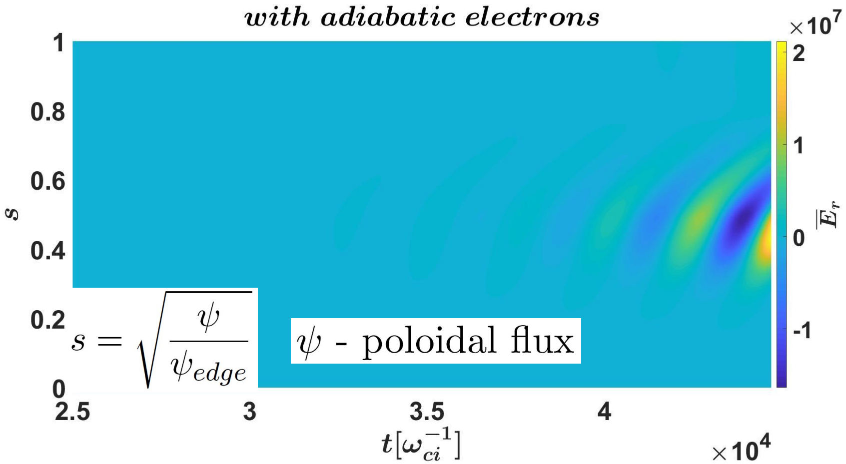

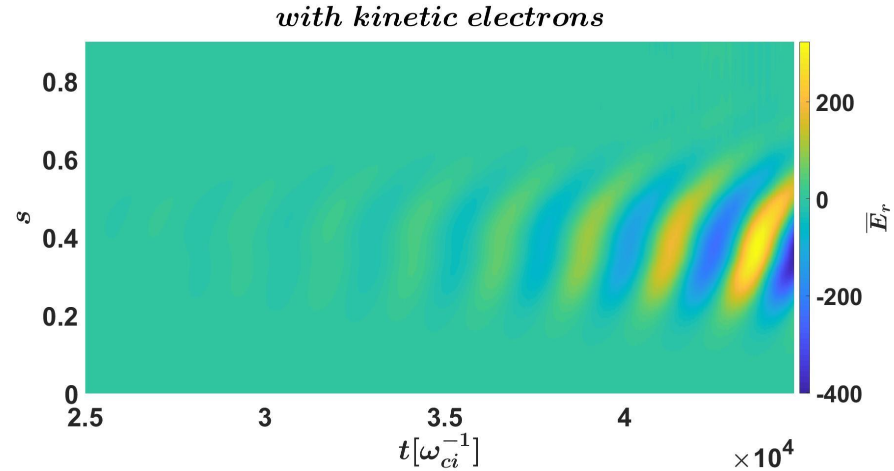

Inclusion of the **drift-kinetic electrons**: **decrease** of the EGAM **growth rate** (by a factor of 2):
-> additional EGAM damping by the electrons
-> increase of the EGAM damping by the thermal ions

Sim. with adiabatic electrons: Sim. with drift-kinetic electrons:

$$\overline{E}_r: \quad \omega[\sqrt{2}v_{th,i}/R_0] = 9.20 \cdot 10^{-1} \pm 3.1 \cdot 10^{-2}, \quad \omega[\sqrt{2}v_{th,i}/R_0] = 9.5 \cdot 10^{-1} \pm 2.3 \cdot 10^{-3},$$

$$MPR: \quad \gamma[\sqrt{2}v_{th,i}/R_0] = +1.62 \cdot 10^{-1} \pm 1.5 \cdot 10^{-3}, \quad \gamma[\sqrt{2}v_{th,i}/R_0] = +8.4 \cdot 10^{-2} \pm 9.3 \cdot 10^{-3},$$

$$thermal\ ions: \quad \gamma[\sqrt{2}v_{th,i}/R_0] = -2.99 \cdot 10^{-1} \pm 2.3 \cdot 10^{-3}, \quad \gamma[\sqrt{2}v_{th,i}/R_0] = -3.8 \cdot 10^{-1} \pm 3.2 \cdot 10^{-2},$$

$$fast\ ions: \quad \gamma[\sqrt{2}v_{th,i}/R_0] = +4.62 \cdot 10^{-1} \pm 1.3 \cdot 10^{-3}, \quad \gamma[\sqrt{2}v_{th,i}/R_0] = +4.6 \cdot 10^{-1} \pm 4.1 \cdot 10^{-2},$$

$$thermal\ ele.: \quad -- \quad \gamma[\sqrt{2}v_{th,i}/R_0] = -3.0 \cdot 10^{-2} \pm 9.6 \cdot 10^{-4}.$$